Determination of a finite-range potential from discrete phase-shift data by inverse scattering

2004 J. Phys. A: Math. Gen. 37 9501

(http://iopscience.iop.org/0305-4470/37/40/012)

INSTITUTE OF PHYSICS PUBLISHING JOURNAL OF PHYSICS A: MATHEMATICAL AND GENERAL

J. Phys. A: Math. Gen. **37** (2004) 9501–9513 PII: S0305-4470(04)79945-X

Determination of a finite-range potential from discrete phase-shift data by inverse scattering

T S Lo[1], S S M Wong[2] and K Young[1]

[1] Physics Department, The Chinese University of Hong Kong, Hong Kong, People's Republic of China
[2] Department of Physics, University of Toronto, Toronto, Canada

E-mail: swong@physics.utoronto.ca

Received 28 April 2004
Published 22 September 2004
Online at stacks.iop.org/JPhysA/37/9501
doi:10.1088/0305-4470/37/40/012

Abstract

A practical method of inverse scattering is proposed to determine a finite-range scattering potential from phase-shift data evaluated at a set of discrete energies. By using the asymptotic behaviour of the phase shifts and the connection between short- and long-wavelength scales, a relatively few input data are found to be adequate. The method works well for repulsive and moderately attractive potentials, useful in many applications.

PACS numbers: 02.30.Zz, 11.80.Et, 03.65.Nk

1. Introduction

A problem of interest in inverse scattering is to reconstruct a central potential $v(r)$ from the phase shift $\delta_\ell(\omega)$ for angular orbital momentum ℓ given by the solution of the scattering equation

$$\frac{\mathrm{d}^2 f_\ell(r,\omega)}{\mathrm{d}r^2} - \left\{\frac{\ell(\ell+1)}{r^2} + v(r) - \omega^2\right\} f_\ell(r,\omega) = 0, \tag{1}$$

where ω^2 is the scattering energy. As $r \to \infty$, the wave function may be written in the form

$$f_\ell(r,\omega) \to \exp\{-\mathrm{i}(\omega r - \ell\pi/2)\} - \exp\{\mathrm{i}[2\delta_\ell(\omega) + \omega r - \ell\pi/2]\}.$$

The phase shift can be deduced from experimental measurements and the question is whether it determines the potential. For sufficiently deep attractive potentials, bound states can exist, and Bargmann [1, 2] and others [3–6] showed that their energies are required as well.

With an infinite set of input information, these classic results in theory solve the problem. In practice, phase-shift data are available only for finite ranges of energies and assumptions must be made about $v(r)$ in order to recover it. One approach is to assume a functional form for $v(r)$ and fit the parameters [7]. Alternatively, one may take $v(r) = v_0(r) + \sum_i c_i v_i(r)$, where

$v_0(r)$ is some known approximation, and the sum expresses the small corrections in terms of a *finite* number of known basis functions $v_i(r)$ and unknown coefficients c_i to be found by perturbative iteration [8, 9]. This implies further assumptions; otherwise, one needs to invoke regulators to control the short-wavelength behaviour [10], a strong assumption on smoothness.

In this work, we consider inversion based on a different premise: that the potential has a finite range a, appropriate in many situations including nuclear physics. For this class of problems, inversion can be achieved using two related sets of input: a finite number of phase shifts sampled at a set of *discrete* points ω_j and the average of $v(r)$ that can be obtained from the asymptotic form of $\delta_\ell(\omega)$. It is known that bound-state information is not always required in recovering the potential in inversion [11] and scattering data alone may provide the complete information. The convenience of not having to rely on bound-state data, nor a functional form nor an approximate initial estimate $v_0(r)$, makes our method complementary to the other approaches. Our result parallels an existing algorithm [12], and the formalism presented here is close to the classic one for spectral inversion [5, 13].

As it stands, the method has several difficulties when the scattering potential is strongly attractive and further improvements are needed. By taking into account the coupling between long and short wavelengths, the applicability of the method has been extended to a much wider range of potentials. This paper shall deal mainly with the extensions made and, to illustrate the essential points, the discussions are restricted to S-waves for simplicity. Generalization to non-zero angular momentum will be given in a separate publication that includes applications to realistic scattering between nuclei. Our method is applicable to a large variety of finite-range potentials; however, it has only been extensively tested on those that tend to zero smoothly as $r \to a$ and some of the details may be specific to this class of potentials.

In section 2, the notation is defined by briefly reviewing the particular inverse-scattering approach followed. Extensions to the method are given in section 3 in terms of test cases that mimic realistic scattering situations. In the conclusion in section 4, we shall also return briefly to the more general situation of angular momentum $\ell > 0$.

2. Formalism

For S-wave and replacing r by x, (1) simplifies to

$$-\partial_x^2 f(x,\omega) + v(x) f(x,\omega) = \omega^2 f(x,\omega) \tag{2}$$

with the potential $v(x)$ defined on a half-line $0 \leqslant x < \infty$ and $v(x > a) = 0$. The boundary conditions are $f(0,\omega) = 0$ and $f'(0,\omega) = 1$ ($' \equiv \partial_x$), the latter a normalization convention. In the place of phase shifts, consider

$$\frac{f'(a,\omega)}{f(a,\omega)} \equiv \mu(\omega) = \omega \cot(\omega a + \delta(\omega))$$

as the input. Subject to technical assumptions about the validity of (i) truncating an infinite matrix system to size N, (ii) invertibility of the resultant $N \times N$ matrix and (iii) taking $N \to \infty$, which are verified in all examples studied, we show that $v(x)$ can be recovered from a discrete set of $\mu(\omega_j)$ together with the average of $v(x)$ given by $\delta(\omega)$ as $\omega \to \infty$.

The algorithm will rely on a known comparison potential $V(x)$, for which the analogue of (2) is

$$-\partial_x^2 F(x,\Omega) + V(x) F(x,\Omega) = \Omega^2 F(x,\Omega),$$

where $F(x,\Omega)$ satisfies the same boundary conditions as $f(x,\omega)$ at $x = 0$ and can be calculated once $V(x)$ is specified.

Following Gel'fand and Levitan [5], $f(x,\omega)$ and $F(x,\omega)$ are related by an integral equation

$$f(x,\omega) = F(x,\omega) + \int_0^x K(x,y)F(y,\omega)\,\mathrm{d}y, \tag{3}$$

where $K(x,y)$, defined for $0 \leqslant y \leqslant x \leqslant a$, unique and independent of ω, satisfies

$$[-\partial_x^2 + \partial_y^2 + v(x) - V(y)]K(x,y) = 0 \tag{4}$$

with the boundary conditions

$$K(x,x) = \frac{1}{2}\int_0^x [v(y) - V(y)]\,\mathrm{d}y, \qquad K(x,0) = 0. \tag{5}$$

The idea, in analogy with spectral inversion [13], is to use the phase shift to determine the Cauchy data

$$H^{(1)}(y) \equiv K(a,y), \qquad H^{(2)}(y) \equiv a\partial_x K(a,y).$$

These serve as the boundary conditions to start a solution of (4), thereby determining $v(x)$ from (5).

2.1. Cauchy data

From (3) and its derivative, and setting $f'(a,\omega) = \mu(\omega)f(a,\omega)$,

$$\partial_x F(a,\omega) + K(a,a)F(a,\omega) + \int_0^a F(y,\omega)\partial_x K(a,y)\,\mathrm{d}y = \mu(\omega)\left[F(a,\omega) + \int_0^a K(a,y)F(y,\omega)\,\mathrm{d}y\right].$$

Thus, similar to (11) of [14][3], we get

$$\int_0^a \mathrm{d}y\,[-\mu(\omega)H^{(1)}(y)F(y,\omega) + a^{-1}H^{(2)}(y)F(y,\omega)] = [\mu(\omega) - H^{(1)}(a)]F(a,\omega) - F'(a,\omega) \equiv h(\omega). \tag{6}$$

The constant $H^{(1)}(a)$ is given by

$$H^{(1)}(a) = K(a,a) = \frac{1}{2}\int_0^a (v - V)\,\mathrm{d}y \equiv \frac{a}{2}(\langle v\rangle - \langle V\rangle),$$

where $\langle\cdots\rangle$ denotes the average over the interval $[0,a]$. The value of $\langle V\rangle$ is known and, for a smooth $v(x)$, a WKB analysis gives

$$\langle v\rangle = -\frac{2}{a}\lim_{\omega\to\infty}\omega\delta(\omega), \tag{7}$$

which can be determined from the asymptotic phase-shift data.

Next, sample $\mu(\omega)$ at $\Omega_j^{(1)}$ and $\Omega_j^{(2)}$ where $F(a,\Omega_j^{(1)}) = 0$ and $F'(a,\Omega_j^{(2)}) = 0$. Evaluating (6) at these two sets of frequencies give

$$\begin{aligned} -\mu_j^{(1)}\langle H^{(1)}|F_j^{(1)}\rangle + a^{-1}\langle H^{(2)}|F_j^{(1)}\rangle &= h_j^{(1)},\\ -\mu_j^{(2)}\langle H^{(1)}|F_j^{(2)}\rangle + a^{-1}\langle H^{(2)}|F_j^{(2)}\rangle &= h_j^{(2)}, \end{aligned} \tag{8}$$

[3] In [14], the corresponding equation is evaluated at the sequence of transmission eigenvalues of the system. Our (6) is valid for any ω, and immediately below we take two sequences of our choice, $\Omega_j^{(1)}$ and $\Omega_j^{(2)}$.

where we have used the shorthand, for $\alpha = 1$ and 2,

$$F_j^{(\alpha)}(y) = F(y, \Omega_j^{(\alpha)}), \qquad \mu_j^{(\alpha)} = \mu(\Omega_j^{(\alpha)}),$$
$$h_j^{(\alpha)} = h(\Omega_j^{(\alpha)}), \qquad \langle G|F\rangle \equiv \int_0^a G(x)F(x)\,\mathrm{d}x.$$

These equations are independent of the normalization of $F_j^{(\alpha)}(y)$ and, henceforth, we let $\langle F_j^{(\alpha)}|F_j^{(\alpha)}\rangle = 1$. As eigenfunctions of self-adjoint systems, each set $\{F_j^{(1)}(y)\}_{j=1}^{\infty}$ and $\{F_j^{(2)}(y)\}_{j=1}^{\infty}$ is complete over $[0, a]$, so we can expand

$$H^{(1)}(y) = \sum_j a_j F_j^{(1)}(y), \qquad H^{(2)}(y) = \sum_j b_j F_j^{(2)}(y). \tag{9}$$

On inserting complete sets, (8) becomes

$$-\mu_j^{(1)} a_j + a^{-1} \sum_{k=1}^{\infty} b_k M_{kj} = h_j^{(1)}, \qquad -\mu_j^{(2)} \sum_{k=1}^{\infty} a_k M_{jk} + a^{-1} b_j = h_j^{(2)}, \tag{10}$$

where

$$M_{kj} \equiv \langle F_k^{(2)}|F_j^{(1)}\rangle$$

is the transformation matrix between the Dirichlet and Neumann bases.

To proceed, we can first eliminate b_j from the two equations in (10) and obtain

$$-\mu_j^{(1)} a_j + \sum_{l=1}^{\infty} N_{jl} a_l = c_j, \tag{11}$$

where

$$N_{jl} = \sum_{k=1}^{\infty} M_{kl} M_{kj} \mu_k^{(2)}, \qquad c_j = h_j^{(1)} - \sum_{k=1}^{\infty} h_k^{(2)} M_{kj} \tag{12}$$

are known quantities. By truncating the system to J equations, the J unknowns a_j are obtained by solving (11) and then b_j from (10). These coefficients in turn give $H^{(1)}(y)$ and $H^{(2)}(y)$ using (9). With these as boundary conditions, $K(x, y)$ is found by solving the partial differential equation (4), and then $v(x) = 2[\mathrm{d}K(x, x)/\mathrm{d}x] + V(x)$ from (5). As a computational algorithm, we use the successive approximation scheme [13]. The convergence is uniform [15] and the solution is unique [16]. These steps are the same as in spectral inversion [6, 13].

Some comments are in order to clarify a few detailed points of the formalism. Firstly, there may not be very much freedom in choosing the sampling frequencies $\Omega_j^{(\alpha)}$. The completeness requirement, coupled with the need to avoid sampling bound states when the potential is sufficiently deep, rules out many possibilities. Secondly, for certain values of a, it is possible that some μ_j become infinite. In such cases, the formalism remains correct as both sides of, for example, (8), can be divided by μ_j. In practice, it is more convenient to avoid the problem by making a slightly different choice of a. Thirdly, it may be difficult to prove that the system (11) is non-singular. However, it is dominated by the diagonal elements and, in all our investigations, we have not encountered the problem in matrix inversion. We note that the basis functions $F_j^{(1)}(y)$ and $F_j^{(2)}(y)$ are complete, so the expansion (9) is rigorous, and the determination of the coefficients a_j and b_j will give the Cauchy data and hence lead to an inversion. The derivation of (11) for the coefficients is also rigorous, so the only remaining issue—which we regard as a reasonable conjecture—is that truncation of (11) at finite N leads to an invertible system, and the limit $N \to \infty$ correctly gives a solution to the original infinite system. In numerical test cases, this procedure has always worked well.

In principle, this solves the inversion problem; in practice, one needs an algorithm that is numerically stable and accurate using only a modest value for J, (half of) the number of input phase shifts. This will be the subject for the rest of this paper.

2.2. Choice of comparison potential

It suffices to consider a constant comparison potential $V(x) = V_0$. Then

$$F_j^{(\alpha)}(y) = (2/a)^{1/2} \sin q_j^{(\alpha)} y,$$

where

$$q_j^{(1)} = j(\pi/a), \qquad q_j^{(2)} = (j-\tfrac{1}{2})(\pi/a)$$

and the frequencies to be sampled are

$$(\Omega_j^{(\alpha)})^2 = (q_j^{(\alpha)})^2 + V_0.$$

With this choice of $V(x)$, the matrix M_{kj} can be evaluated explicitly:

$$M_{kj} = (-1)^{j+k+1} \frac{2}{\pi} \frac{j}{(k-1/2)^2 - j^2}.$$

For any choice of $V(x)$, each of the sets $\{F_j^{(1)}\}$ and $\{F_j^{(2)}\}$ remains complete, and the above algorithm works in theory. In practice, two considerations limit the choice. Firstly, the reference potential cannot be strongly attractive, to ensure $(\Omega_j^{(\alpha)})^2 > 0$; otherwise one would need to sample $\delta(\omega)$ at imaginary values of ω. Secondly, if $V(x)$ is very different from $v(x)$, $f(x,\omega)$ and $F(x,\omega)$ are no longer close to each other and the integral transform (3) differs substantially from unity. In such cases, the solution may become numerically unstable. Similar considerations apply in spectral inversion, where one typically chooses $\langle V \rangle = \langle v \rangle$. The second requirement cannot be satisfied when $v(x)$ is strongly attractive and other methods are needed to stabilize the calculation. This is addressed in section 3.

2.3. Comparison with spectral inversion

The approach we take here has a number of significant differences compared with the classic method for spectral inversion [5]. In spectral inversion, the input data for the unknown potential $v(x)$ are evaluated at the Dirichlet and Neumann eigenvalues $\omega_j^{(\alpha)}$, leading to hybrid functions $F^{(\alpha)}(x, \omega_j^{(\alpha)})$—the functional form is determined by $V(x)$, but the values of ω are determined by $v(x)$. Thus, their completeness is a nontrivial matter [17], and relies on $V(x)$ and $v(x)$ being close; these functions are not orthogonal either. The resulting equations, roughly corresponding to (8), are on the other hand decoupled and simple. In our present case, the corresponding functions are $F^{(\alpha)}(x, \Omega_j^{(\alpha)})$—both the functional form and the values of ω are determined by $V(x)$; so they are trivially complete and orthogonal. However, the two equations in (8) become coupled, and the non-diagonal transformation matrix M_{kj} makes it necessary to consider the truncation with care.

3. A practical algorithm

The method outlined in the previous section to find the underlying scattering potential from phase-shift data works in principle. Difficulties in applications, however, arise when the potential is strongly attractive and the number of available input phase shifts is limited. We shall illustrate here the necessary extensions in practical situations using specific examples.

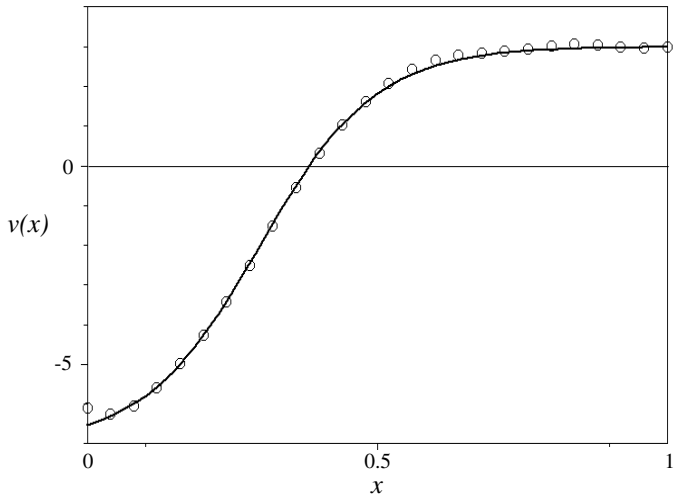

Figure 1. A potential with zero mean reconstructed from phase shifts. Circles are the calculated results for $v(x)$ using $J = 4$ terms in the inversion. The result at $x = 0$ is greatly improved by increasing J to 8 (not shown). For comparison, the original potential $u(x)$ is indicated by the solid line.

For this purpose, we use as input a set of $\delta(\omega)$ generated from some known potential $u(x)$. By comparing the recovered $v(x)$ with the original $u(x)$, it is possible to see how well the method works and the improvements required. To obtain the input phase shifts, (2) is solved numerically using a fourth-order Runge–Kutta method, with a grid size $10^{-5}a$, where $[0, a]$ is the range of interest. The matrix equations involved have dimension J. The input thus consists of only $2J$ values of $\delta(\omega)$ together with the value of $\langle v\rangle$ obtained from the asymptotic phase shift.

Without loss of generality we take $a = 1$. A truncated Woods–Saxon potential with a shift v_0 is used,

$$u(x) = \left\{ \frac{U_0}{1 + \exp[(x-R)/s]} + v_0 \right\} \Theta(1-x),$$

where R is the radius and s the surface diffuseness of the well. The unit step function $\Theta(1-x)$ ensures that $u(x > 1) = 0$. The form of $u(x)$ is close to that encountered in nuclear scattering, for example, in [7], and the comparisons should provide useful guidance for actual applications.

To highlight the importance of both the need and the means to reduce the number of necessary input phase shifts, three test cases with $U_0 = -10$, -40 and -80 are discussed below. In all cases, $R = 0.3$ and $s = 0.1$.

3.1. Examples with $\langle v\rangle \geqslant 0$

As a start, let us reassure ourselves that the inversion method does work for relatively weak potentials by applying to a case with $U_0 = -10$, $R = 0.3$, $s = 0.1$, very similar to those normally used to demonstrate new inversion algorithms. Figure 1 shows the results with v_0 adjusted to make $\langle u\rangle = 0$. Even with $J = 4$ terms the inversion is very accurate (except for $x \approx 0$). With more terms, for example, $J = 8$, even the $x = 0$ result is satisfactory. We

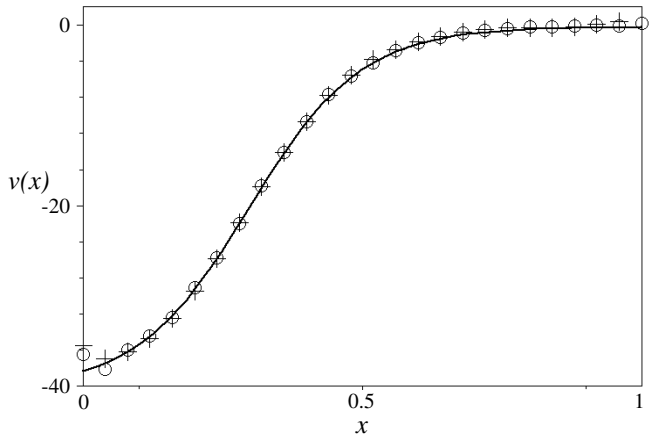

Figure 2. Inversion for a moderately attractive potential, $U_0 = -40$ and $v_0 = 0$; crosses are the results with $J = 20$, $\alpha_1 = -6.096$ and $\alpha_3 = 0$; circles, those with $J = 8$, $\alpha_1 = -6.096$ and $\alpha_3 = 115.6$. For comparison, the original potential is indicated by the solid line.

conclude from the example that, for smooth, shallow potentials, inversion is a relatively simple problem. We shall return at the end of this section to a broader category of potentials.

3.2. Moderately attractive potentials and an improved algorithm

In realistic applications, the potential is usually stronger and most inversion techniques have difficulties in such cases. To demonstrate this point, we show in figure 2 a deeper Woods–Saxon potential with $U_0 = -40$ (and the same $R = 0.3$ and $s = 0.1$) and $v_0 = 0$. Here $\langle v \rangle$ is significantly negative and the potential is sufficiently deep to have one bound state. With $V_0 = 0$, it takes $J \gg 100$ before any reasonable results can be obtained (not shown). Only very limited improvements can be achieved by adjusting the comparison potential $V(x)$: since $v(x)$ is attractive, a negative $V(x)$ should be used. On the other hand, $V(x)$ cannot be made too attractive, otherwise there will be bound states (and, thus, the need to sample imaginary frequencies, as mentioned earlier). The alternative of greatly increasing the value of J is not desirable either, as it implies the need for input data at very high scattering energies.

Let us re-examine (11). With only $2J$ input quantities, the infinite set of equations, as well as the sums in these equation, must be truncated to J and this is valid only if

$$a_j \approx 0 \tag{13}$$

for $j > J$. In appendix A, we show that, as $j \to \infty$,

$$a_j = (-1)^{j+1}\sqrt{2}\frac{\alpha_1}{j\pi} + \mathrm{O}(j^{-3}), \tag{14}$$

where

$$\alpha_1 = \tfrac{1}{2}(\langle v \rangle - \langle V \rangle). \tag{15}$$

Thus $a_j \sim j^{-3}$ if $\langle v \rangle$ and $\langle V \rangle$ are matched, but $a_j \sim j^{-1}$ otherwise. In the latter case, truncating the sums (9) using a small J value would be inaccurate. Since it is not always practical to use larger J values, one needs to devise a way to 'correct' for the higher-order ($j > J$) phase shifts we do not wish to include explicitly as input data.

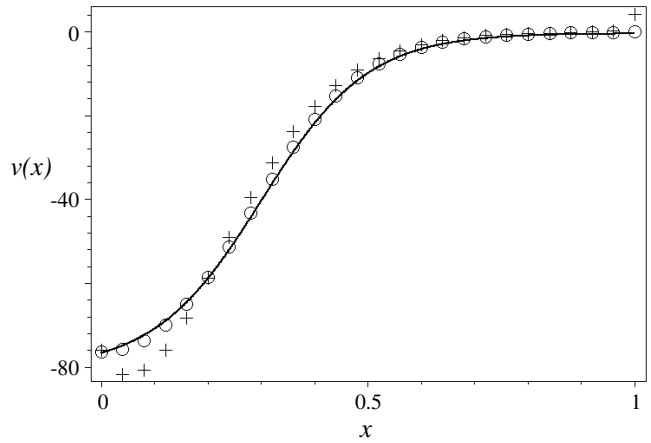

Figure 3. Inversion for a potential with $U_0 = -80$ and $v_0 = 0$. Crosses are the results with $\alpha_1 = -12.19$, $\alpha_3 = 0$ and $J = 70$; circles with $\alpha_1 = -12.19$, $\alpha_3 = 687.19$ and $J = 30$. The original potential $u(x)$ is shown as the solid line for comparison.

To this end, let us define

$$\bar{a}_j \equiv (-1)^{j+1}\sqrt{2}\frac{\alpha_1}{j\pi}, \qquad \Delta a_j \equiv a_j - \bar{a}_j.$$

In terms of Δa_j, (11) becomes

$$-\mu_j^{(1)}\Delta a_j + \sum_{l=1}^{\infty} N_{jl}\Delta a_l = c_j + \mu_j^{(1)}\bar{a}_j - \sum_{l=1}^{\infty} N_{jl}\bar{a}_j.$$

Truncation of the sum on the left-hand side of the equation now only requires

$$\Delta a_l \approx 0$$

for $l > J$, a weaker condition compared with (13) since $\Delta a_j \sim j^{-3}$. Moreover, the infinite sum for $H^{(1)}(y)$ in (9) can be written as

$$\sum_{j=1}^{\infty} a_j F_j^{(1)} = \sum_{j=1}^{\infty} \bar{a}_j F_j^{(1)} + \sum_{j=1}^{\infty} \Delta a_j F_j^{(1)},$$

where the first term can be evaluated analytically (appendix B). Since only the second sum needs to be truncated to J, the error is much smaller. The result of the new scheme with $J = 20$ and $\alpha_1 = -6.096$ [$=\frac{1}{2}\int_0^1 u(x)\,\mathrm{d}x$] is shown as crosses in figure 2. The improvement achieved with only one extra degree of freedom α_1 is quite significant, demonstrating the need to correct for large-j terms.

3.3. More than one asymptotic coefficient

For deeper potentials, the use of a single asymptotic coefficient, as done in the previous example, is still inadequate. To illustrate this point, we consider next a case with $U_0 = -80$ (and the same $R = 0.3$, $s = 0.1$ and $v_0 = 0$). With $\alpha_1 = -12.19$ and a comparison potential $V_0 = 0$, the result, shown as crosses in figure 3, is inaccurate even with as many as $J = 70$ terms.

To make further progress, we generalize (14) by using K coefficients[4]. Define

$$\bar{a}_j = (-1)^{j+1}\sqrt{2}\sum_{k=1}^{K}\frac{\alpha_{2k-1}}{(j\pi)^{2k-1}}, \tag{16}$$

where α_1 is known from (15) and (7). For arbitrary potentials, there does not seem to be any natural way to determine $\alpha_3, \ldots, \alpha_{2K-1}$ *a priori* as done for α_1. The alternative is to obtain their values self-consistently. Let us illustrate this point with $K = 2$. That is, we include, besides α_1, an additional coefficient α_3. Starting with an arbitrary initial estimate of α_3 (e.g. $\alpha_3 = 0$), the coefficients Δa_j and, hence a_j, are solved by truncating the matrix equations after J terms. The values of a_j for higher j values, say $J' \leqslant j \leqslant J$, are fitted to (16) to obtain an improved value α_3'. The calculations are repeated using α_3'. The procedure defines a mapping $\alpha_3' = T(\alpha_3)$ whose fixed point is sought.

Once we have the correct value of α_3, it is used in conjunction with that of α_1 to obtain coefficients a_j and b_j, and thence the Cauchy data $H^{(\alpha)}(y)$, in a manner similar to section 3.2. The explicit expressions are given in appendix B. As seen in figure 3, the inversion result with α_3 included is far superior to those without, even though J is much reduced. The same is true for the $U_0 = -40$ case in figure 2: by introducing the α_3 coefficient the J value is reduced from 20 to 8 without sacrificing the accuracy.

It is useful to give some heuristic estimates for the improvement expected in the presence of coefficients α_1, α_3, etc. The error in using a naive truncation ($K = 0$) after J_0 terms is $\sim |\alpha_1|(J_0\pi)^{-1}$; the error in using K parameters up to α_{2K-1} and truncating after J_K terms is $\sim |\alpha_{2k+1}|(J_K\pi)^{-2K-1}$. These would be comparable in accuracy if

$$|\alpha_1|(J_0\pi)^{-1} \sim |\alpha_{2K+1}|(J_K\pi)^{-2K-1}.$$

Using (A.2), this reduces to

$$(J_0\pi)^{-1} \sim (a/\beta)^{2k}(J_K\pi)^{-2K-1},$$

where β is the shortest length scale in the problem (see appendix A).

Consider the example used in figure 3. The value of $\beta \sim 0.1$, giving $a/\beta \sim 10$. Since the case does not quite satisfy the $J \gg a/\beta$ criterion, the estimates can only provide a rough guidance. To reach the same accuracy as achieved by $J_2 = 30$ shown in the figure, it will take J_1 on the order of several hundred (rather than 70 represented by the crosses). If α_1 is also taken to be zero, it would take $J_0 \sim |\alpha_1|/|\alpha_3|J_2^2\pi^2$—around a few times 10^4—to reach even the level given by $J_1 = 70$. (The same arguments show also that it would take $J_0 \gg 100$ for any success in the $U_0 = -40$ case of figure 2.) For deeper potentials, it may be necessary to go to $K = 3$ and higher to keep the input phase shifts to reasonable numbers.

The importance of keeping the J value to a minimum may be seen from the following arguments. With J terms, the highest energy E at which phase-shift data are required would be

$$E \sim \frac{\hbar^2}{2m}\left(\frac{J\pi}{a}\right)^2.$$

Using $mc^2 = 2000\,\mathrm{MeV}$ and $a = 10\,\mathrm{fm}$, appropriate for α–α scattering, yields $E \sim J^2\,\mathrm{MeV}$. Since nuclear scattering experiments, for example, are seldom carried out to GeV energy scales, either because of accelerator limitations or difficulties in resolving the elastic results from the large number of open inelastic channels, one is limited to $J \sim 30$. The possibility

[4] It is readily shown from the partial differential equation satisfied by $K(x, y)$ that this expansion has only odd powers $2k - 1$ and the signs alternate with j.

of approximating the large-j terms using asymptotic coefficients α_k is therefore essential in applications.

For potentials that are oscillatory in x or possess singularities, e.g. at $x = 0$, it is clear that more input data are needed to specify their detailed structures. On the other hand, even with limited information, the Cauchy data should be able to indicate the presence of such behaviour in terms of the j dependence of a_j, which should itself give warning when more data are needed.

4. Conclusion

We have shown that a finite-range potential $v(x)$ can in principle be recovered from the phase shift $\delta(\omega)$ sampled at a reasonable number of discrete values ω_j, together with its asymptotic behaviour as $\omega \to \infty$. The amount of available input information is an important practical consideration in inversion studies. Often, scattering measurements can only be carried out over a finite range of energies and thus the experimental input for recovering the underlying potential is limited. The need of input to very high scattering energies may be one reason why inversion techniques are seldom used directly in certain applications.

In terms of our approach, the number of input phase shifts translates into the number of coefficients a_j and b_j that can be calculated to determine the Cauchy data $H^{(\alpha)}(y)$, the boundary conditions to solve the partial differential equation (4) and thence the potential $v(x)$. Since the higher-order coefficients cannot be simply ignored, we make use of the coupling between short and long wavelengths to generate the necessary corrections to the Cauchy data and this allows recovery of potentials that are sufficiently deep to contain one or more bound states. It is well known that the formal inversion problem has a unique solution [16], but the exclusion of high-energy data in effect cuts off information on short-wavelength scales. Therefore, there can be other solutions that differ only in the short-wavelength features[5], but these differences are not usually significant physically.

In fact, our method is complementary to other inversion approaches. Fitting is useful where the form of the potential is available and iterative perturbation is powerful when $v(x)$ is approximately known. In our approach, $v(x)$ is assumed to have finite support, but otherwise no assumptions are made about either the functional form or the value of $v(x)$. (The mean value $\langle v \rangle$ is needed, but is determined from the data and not assumed *a priori*.) It could therefore provide a different perspective, especially in exploring degrees of freedom that might otherwise be implicitly ruled out.

We have restricted attention in this paper to S-waves so as to give a clear illustration of the method itself in the simplest context. The only additional work for $\ell > 0$ is the purely technical one related to the angular momentum barrier term in (1). This, in turn, requires the addition of x^{-2} and y^{-2} terms in (4). As a result, the numerical solutions to the partial differential equation must be handled with more care. On the other hand, since the angular momentum barrier is repulsive, the effective potential for an attractive well, $v(r) + \ell(\ell+1)/r^2$, is shallower than the corresponding S-wave case, making it easier to carry out the inversion calculation itself. (For repulsive potentials, there are no problems either way.) As a first application, we are considering α–α scattering where extensive data are available. Other spin-0 scattering can also be examined in the same way and the results will be presented separately with the necessary specialization to the nuclear case. Extensions to non-spin-0 scattering are also under investigation. Inverse scattering is, however, a problem encountered in many fields

[5] If we use say $2J$ data points, then consider a potential that is the one inverted plus a small correction, where the latter is a Fourier series on $[0, a]$ with L coefficients, with $L > 2J$, clearly the coefficients cannot be uniquely determined.

other than nuclear physics and the algorithm presented here has much wider implications than the immediate applications we have in mind.

Technically, it is more difficult to obtain the potential shape for $r \approx 0$, as $F_\ell(r)$ are small near the origin for $\ell > 0$, and any numerical uncertainties in the calculations are likely to be amplified. However, the shape very close to the origin is unimportant in practical applications, as the potential near the origin is not well sampled by the wavefunction except at very high energies and, hence, does not significantly affect any physical quantities except at such energies.

Acknowledgments

The authors acknowledge the support of Hong Kong Research Grant Council (CUHK4006/98P) and that of Natural Science and Engineering Council of Canada to one of us (SSMW).

Appendix A. Evaluation of α_k

Inverting the first member of (9) and putting in the explicit form of the eigenfunctions $F_j^{(\alpha)}(y)$, we have for $a = 1$,

$$a_j = \sqrt{2} \int_0^1 \sin(j\pi y) H^{(1)}(y)\, \mathrm{d}y.$$

Assuming $H^{(1)}(y)$ is smooth, the large-j asymptotics are related to its behaviour at the end-points of the interval. Integrating by parts gives

$$\alpha_1 = H^{(1)}(1) = K(1,1) = \tfrac{1}{2}(\langle v \rangle - \langle V \rangle),$$

where the last step follows from (5). More generally, further integrations by parts yield

$$\alpha_{2k+1} = (-1)^k \frac{\mathrm{d}^{2k} H^{(1)}(y=1)}{\mathrm{d}y^{2k}}. \tag{A.1}$$

The contributions at the lower limit vanish by virtue of (4) and its derivatives at $y = 0$.

All indications show that the derivatives in (A.1) scale nearly geometrically in k,

$$\frac{\mathrm{d}^k H^{(1)}(y=1)}{\mathrm{d}y^k} \sim H_0 \rho^k.$$

This is confirmed numerically to be accurate up to at least the fourth-order derivatives. For the example shown in figure 3, we find $\rho \sim 10$. The order-of-magnitude of ρ can be understood from a heuristic argument. There are two possible short length scales in the problem. The first, β_1, is given by the variation of $v(x)$. For a Woods–Saxon potential, we have $\beta_1 = s$, the surface diffuseness. Second, there is the wavelength $\beta_2 \sim v^{-1/2}$ given by the typical depth of $v(x)$. In general, one can expect the shortest length scale in $K(x, y)$ and, hence, $H^{(1)}(y) = K(a, y)$, to be given by $\beta = \min(\beta_1, \beta_2)$. Therefore $\rho \sim \beta^{-1}$. Thus one finds the estimate

$$\alpha_{2k+1} \sim (-1)^k (a/\beta)^{2k} \alpha_1, \tag{A.2}$$

where factors of a have been inserted for dimensional consistency.

Appendix B. Evaluation of infinite sums

Let $\bar{a}_j$ be given by (16) with two terms α_1 and α_3. Consider the first sum in (16) which involves

$$\sum_{j=1}^{\infty} \frac{(-1)^{j+1}}{(j\pi)^k} \sin(j\pi y)$$

for $k = 1, 3$. These can be evaluated analytically giving the result

$$\sum_{j=1}^{\infty} \bar{a}_j F_j^{(1)} = (\alpha_1 + \alpha_3/6)y - (\alpha_3/6)y^3.$$

Other infinite sums may be handled in a similar way. For example, for N_{jl} in (12), we can first rewrite $\mu_j^{(2)}$ as

$$\mu_j^{(2)} = \gamma_0 + \frac{\gamma_2}{(j-1/2)^2\pi^2} + \Delta\mu_j^{(2)},$$

where $\gamma_0 = H^{(1)}(a)$ is known. Inserting the result into (12), the γ_0 term is summed to infinity, giving

$$\sum_{k=1}^{\infty} M_{kj} M_{kl} \gamma_0 = \delta_{jl}\gamma_0.$$

The value of γ_2 is fitted to the data to make the last term $\sim j^{-4}$ and the term proportional to γ_2 can be summed numerically to as many terms as needed. The $\Delta\mu_j^{(2)}$ contribution is summed to $j = J$. In this way terms with $j > J$ in the infinite sums are replaced by $\mathrm{O}(j^{-2})$ estimates.

Similarly, in the place of (9),

$$H^{(2)}(y) = \xi y + \sum_j \Delta b_j F_j^{(2)}(y)$$

with ξ and Δb_j given by

$$b_j = (-1)^{j+1}\sqrt{2}\frac{\xi}{(j-1/2)^2\pi^2} + \Delta b_j.$$

The value of ξ is obtained by fitting b_j and the resulting Δb_j is found to be $\mathrm{O}(j^{-4})$ asymptotically.

References

[1] Bargmann V 1949 *Phys. Rev.* **75** 301
[2] Bargmann V 1949 *Rev. Mod. Phys.* **21** 488
[3] Faddeev L D 1959 *Usp. Mat. Nauk.* **14** 57
Seckler B 1963 *J. Math. Phys.* **4** 72 (Engl. Transl.)
[4] Dyson F J 1976 *Essays in Honor of Valentine Bargmann* (Princeton, NJ: Princeton University Press)
[5] Levitan B M 1987 *Inverse Sturm–Liouville Problems* (Utrecht: VNU Science Press)
[6] Chadan K, Colton D, Päivärinta L and Rundell W 1997 *An Introduction to Inverse Scattering Problems* (Philadelphia, PA: SIAM)
[7] See, e.g., Koning A J and Delaroche J P 2003 *Nucl. Phys.* A **713** 231
[8] Mackintosh R S and Cooper S G 1998 *J. Phys. G: Nucl. Part. Phys.* **24** 1599
[9] Wong S S M and Young K 2000 *J. Phys. G: Nucl. Part. Phys.* **26** 1655
[10] Sun C-P, Young K and Zou J 1999 *J. Phys. A: Math. Gen.* **32** 3833
[11] Ramm A G 1998 *Phys. Lett.* A **242** 215
[12] Rundell W and Sacks P 1994 *J. Comput. Appl. Math.* **55** 325

[13] Rundell W and Sacks P E 1992 *Math. Comput.* **58** 161
[14] McLaughlin J R, Polyakov P L and Sacks P E 1994 *SIAM J. Appl. Math.* **54** 1203
[15] Sacks P E 1988 *Inverse Problems* **4** 1055
[16] Suzuki T 1985 *J. Fac. Sci. Univ. Tokyo Sect. IA Math.* **32** 223
[17] Levinson N 1940 *Gap and Density Theorems* (Providence, RI: American Mathematical Society) (cited in [6])